

Identifying the non-linearities in the period-luminosity relations of Cepheids

Julien Dassa-Terrier^{1*} and David Valls-Gabaud^{1,2}

¹LERMA, Observatoire de Paris

²Institute of Astronomy, Cambridge

*julien.dassa-terrier@obspm.fr

The period-luminosity relations of Cepheids are essential to characterize the second step of the cosmological distance ladder. However, the possible non-linearity and breaking points around a period of 10 days have important consequences for their use. Here we summarize two statistical techniques aimed at identifying these points and quantifying the implied non-linearities. The efficiency of these methods is discussed with observational samples from the Magellanic Clouds and M31.

1. Period-luminosity relation and the cosmological distance ladder

Essential dates:

- **1838** — Bessel measures the parallax of 61 Cygni.
- **1912** — Leavitt discovers the Period-Luminosity relation, also called Leavitt Law (LL): $M = a \cdot \log P + b$, which correlates the period and absolute mean magnitude of Cepheids.
- **1924** — Hubble uses the LL to calculate the distance of the galaxy M31.
- **1968** — Sandage and Tammann introduce the period-luminosity-colour relation which adds a colour element to the LL:

$$M = \alpha \cdot \log P + \beta \cdot (B - V) + \gamma$$

I. Parallax
in Milky
Way

II. Cepheids
in local
Universe

III. Type Ia
supernovae
in distant
galaxies

Hubble
constant

The calibration of the LL is a very important, debated topic, essential to find the distance modulus: $\mu = m - M = 5 \log(d) - 5$, where m is the apparent magnitude and d the distance to the star.

Cepheids being standard candles, the slope a of the LL can be found by observing the magnitude and period of a group of Cepheids (see figure 1) while the zero point b must be found using galactic Cepheids with known distances.

Riess et al. (2012) propose one of the most recent calibrations using data from HST (PHAT) and CFHT (POMME survey) applied to the distance measurement of M31. They estimate M31 distance to be $752 \pm 27 \text{ kpc}$ and find $H_0 = 75.4 \pm 2.9 \text{ km s}^{-1} \text{ Mpc}^{-1}$.

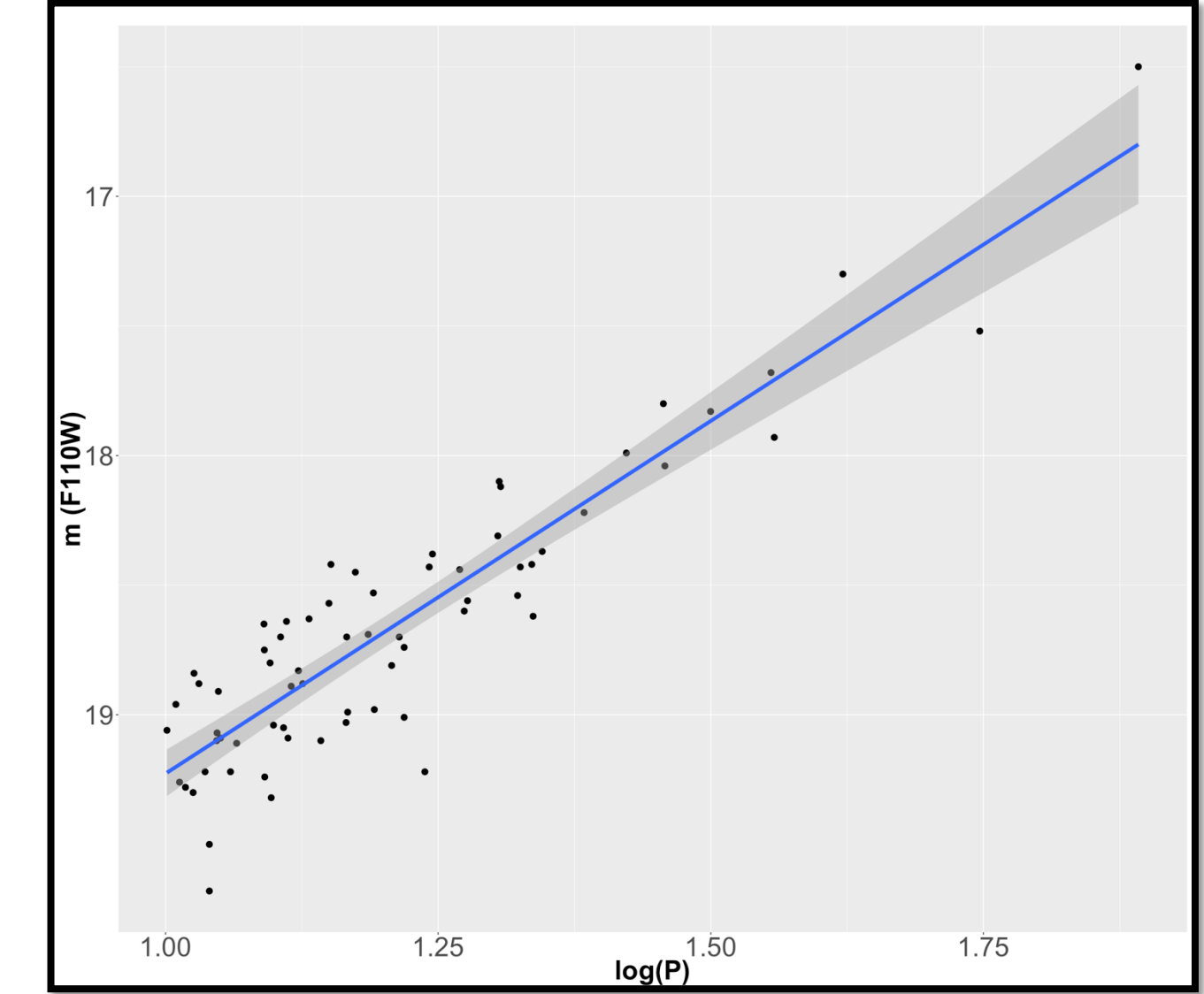


Figure 1 – The LL for 68 classical Cepheids from the POMME survey. The law shows a linear behaviour for $\log(P) \geq 1$ (Riess et al., 2012).

2. Non-linearities and breaking points

Recent studies, including Tammann et al. (2002), Ngeow & Kanbur (2009) and Kodric et al. (2015), strongly imply that the LL shows a non-linear behaviour in the LMC, SMC and M31 with the presence of a breaking points at $P = 10 \text{ d}$. This breaking point was already suggested by Kakurkin in 1937 (Ngeow et al. , 2005).

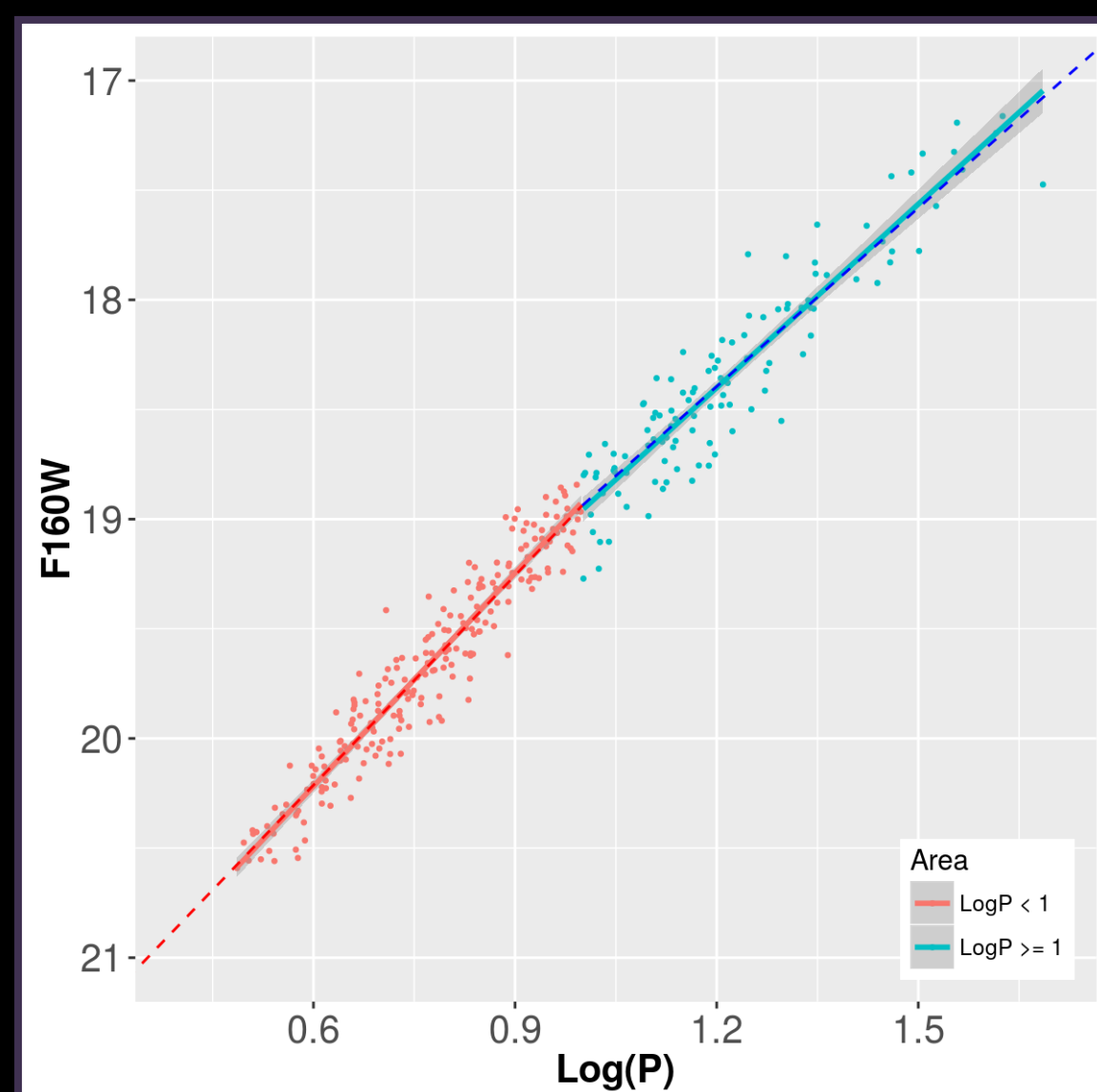


Figure 2 – The LL breaking point for 319 fundamental mode (FM) Cepheids in the galaxy M31 as shown in Kodric+ (2015).

This is an empirical observation and a controversial topic. Several solutions have been suggested such as: the dependence of the LL on metallicity (Caputo et al., 2000; Marconi et al. , 2005) or the interaction of stellar photosphere with the hydrogen ionization front (Ngeow & Kanbur, 2009).

This behaviour might have a strong impact on the slope of the LL, hence on the distance modulus and H_0 calculations. Kodric et al. (2015)

Without a strong consensus on one physical explanation, the non-linear behaviour of the LL remains largely studied through statistical analysis, particularly the F-test (Ngeow et al., 2004).

3. Statistical tools

We suggest two alternative approaches:

- the frequentist Bai and Perron's method BP (Bai & Perron, 2003),
- the Bayesian Barry and Hartigan's method bcp (Barry & Hartigan, 1993; Erdman & Emerson, 2007).

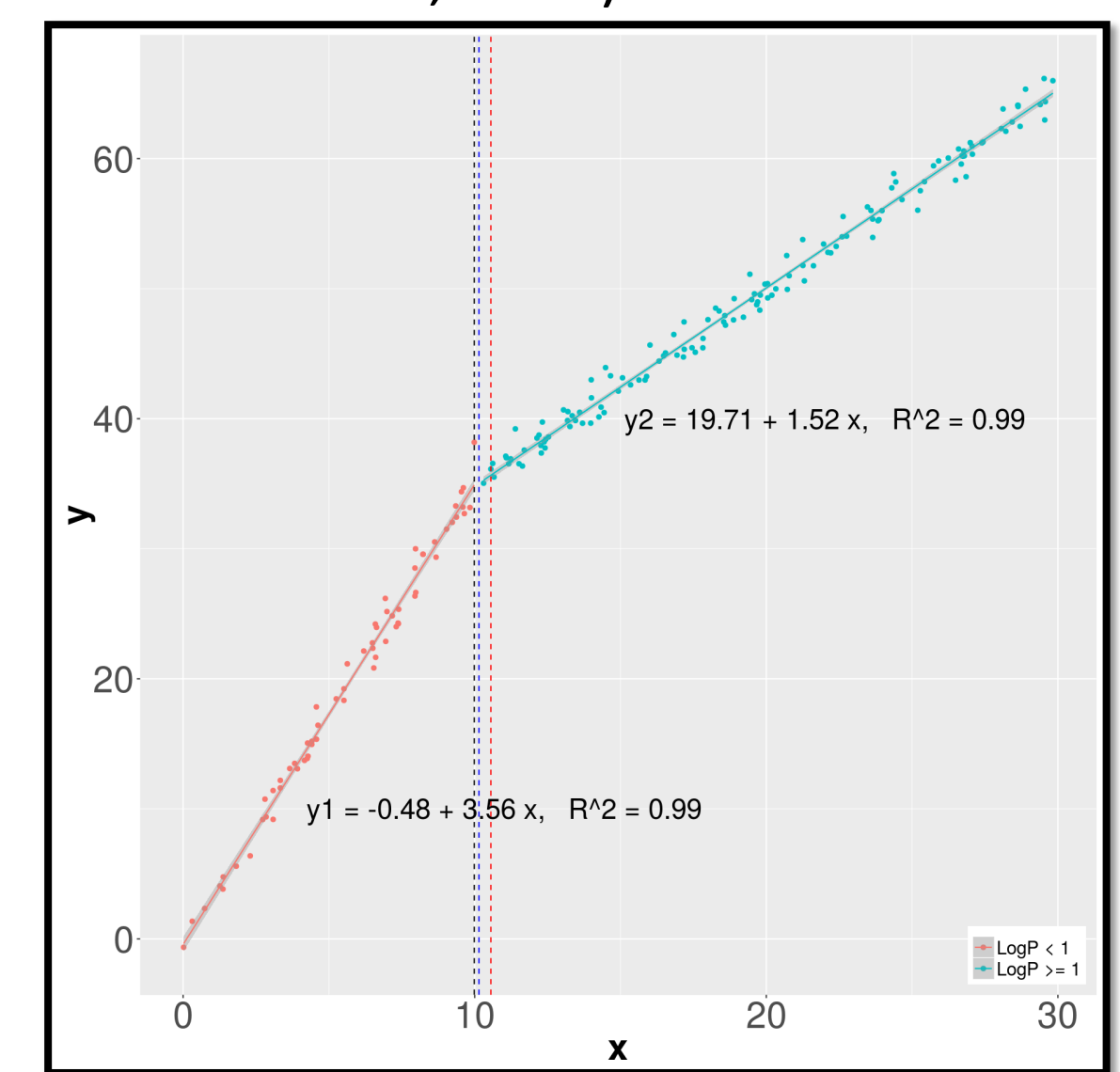


Figure 3 – A simulated sample of $n = 200$ objects, with two continuous linear function of slope $a_1 = 3.5$ and $a_2 = 1.5$. The breaking point is $\tau_x = 10$. Dashed lines show the breaking points found for BP (blue), two different uses of bcp (red and black). y_1 and y_2 are the two functions fitted for the best breaking point found.

4. Simulations and tests

- The model proposed by Kodric et al. (2015), displayed in table 1, serves as a foundation to build our simulations.
- We choose N the number of objects.
- We choose σ the added noise to the magnitude.
- τ , the breaking point, is always $\log_{10}(P) = 1$.

| Band | Slope $\log(P) \leq 1$ | Slope $\log(P) > 1$ | Intercept $\log(P) = 1$ |
|-------|------------------------|---------------------|-------------------------|
| F110W | $-3.028(0.078)$ | $-2.433(0.105)$ | $19.455(0.021)$ |

Table 1 – Function fitted on an observational sample of fundamental mode Cepheids of M31 by Kodric et al. (2015) for the F110W filter.

Figure 4 – Breaking points found by both BP and bcp methods for different values of N and σ . As the bcp method provides us with a probability for each object to be a breaking point, we compute the value of the breaking point with two different methods displayed as bcp1 and bcp2. The latter gives better results particularly for $\sigma = 0.4$, where bp and bcp1 show difficulties to identify a breaking point.

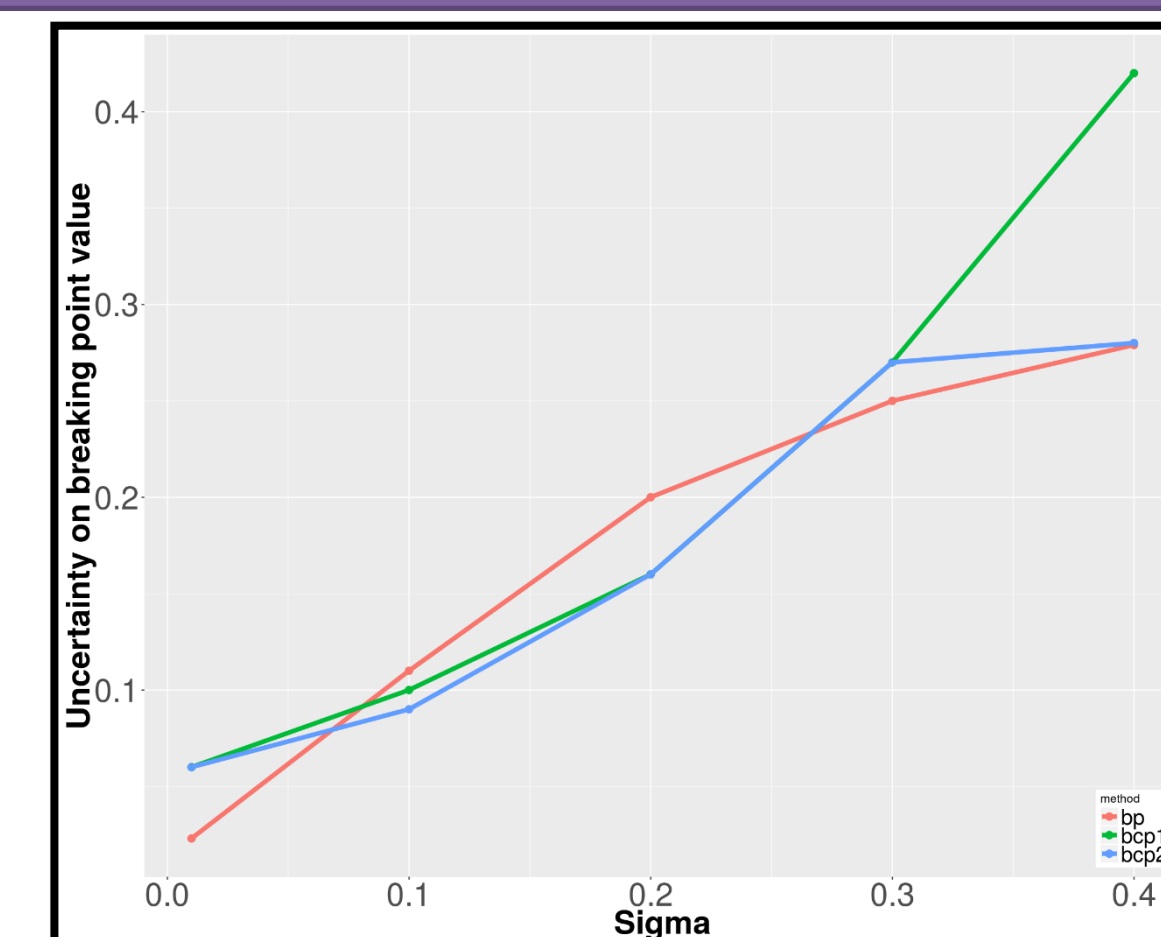
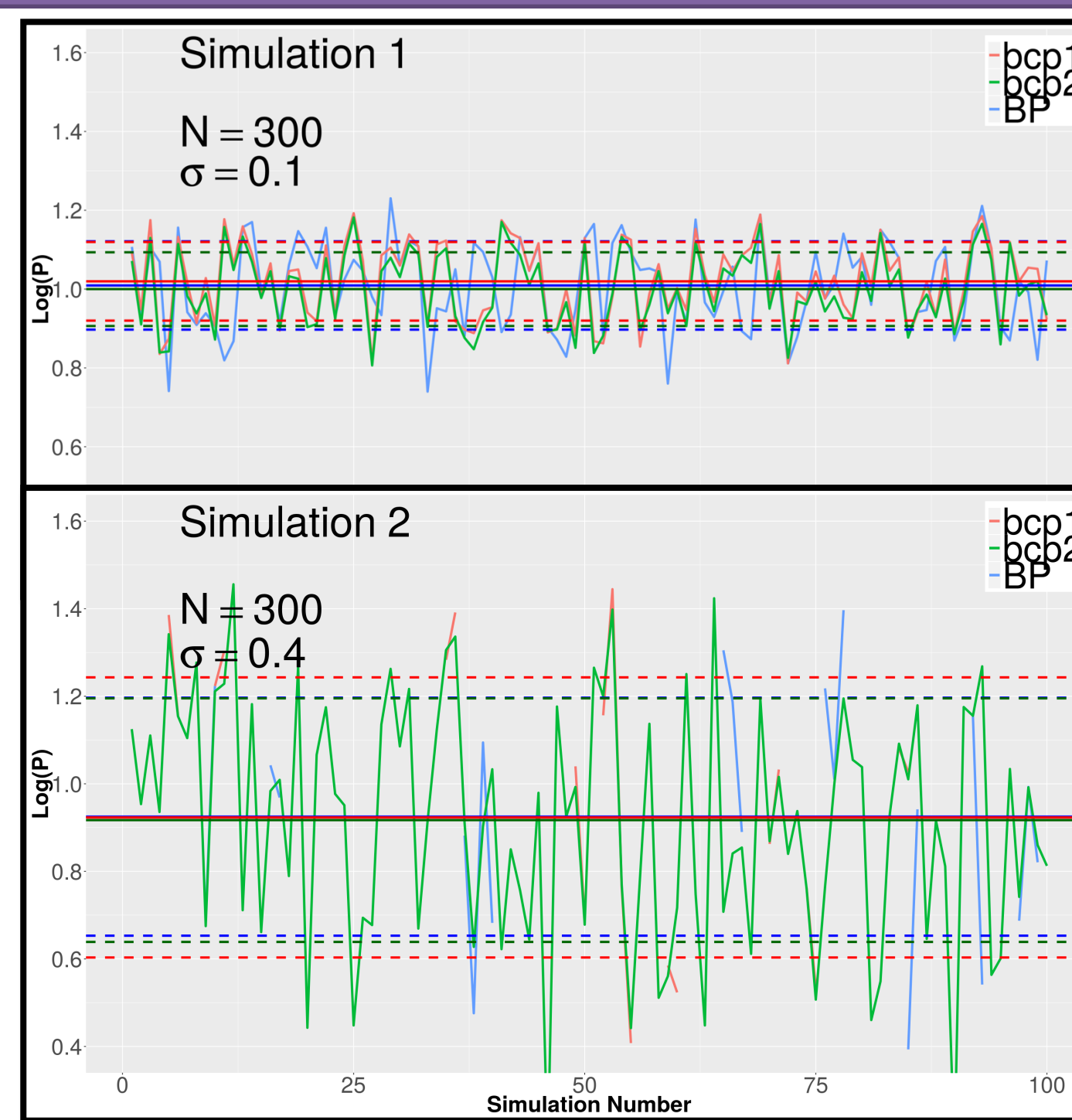


Figure 5 – The uncertainty on the breaking point value grows significantly with respect to the sigma added to the simulated samples. While the bcp methods have lower accuracy than the BP method at small sigma, bcp1 show a particularly strong rise in uncertainty at higher values of sigma.

- The efficiency of the methods is strongly dependant on the noise added.
- A perturbation of $\sigma = 0.4$ gives to the sample a dispersion similar to observations.

5. Applications to M31

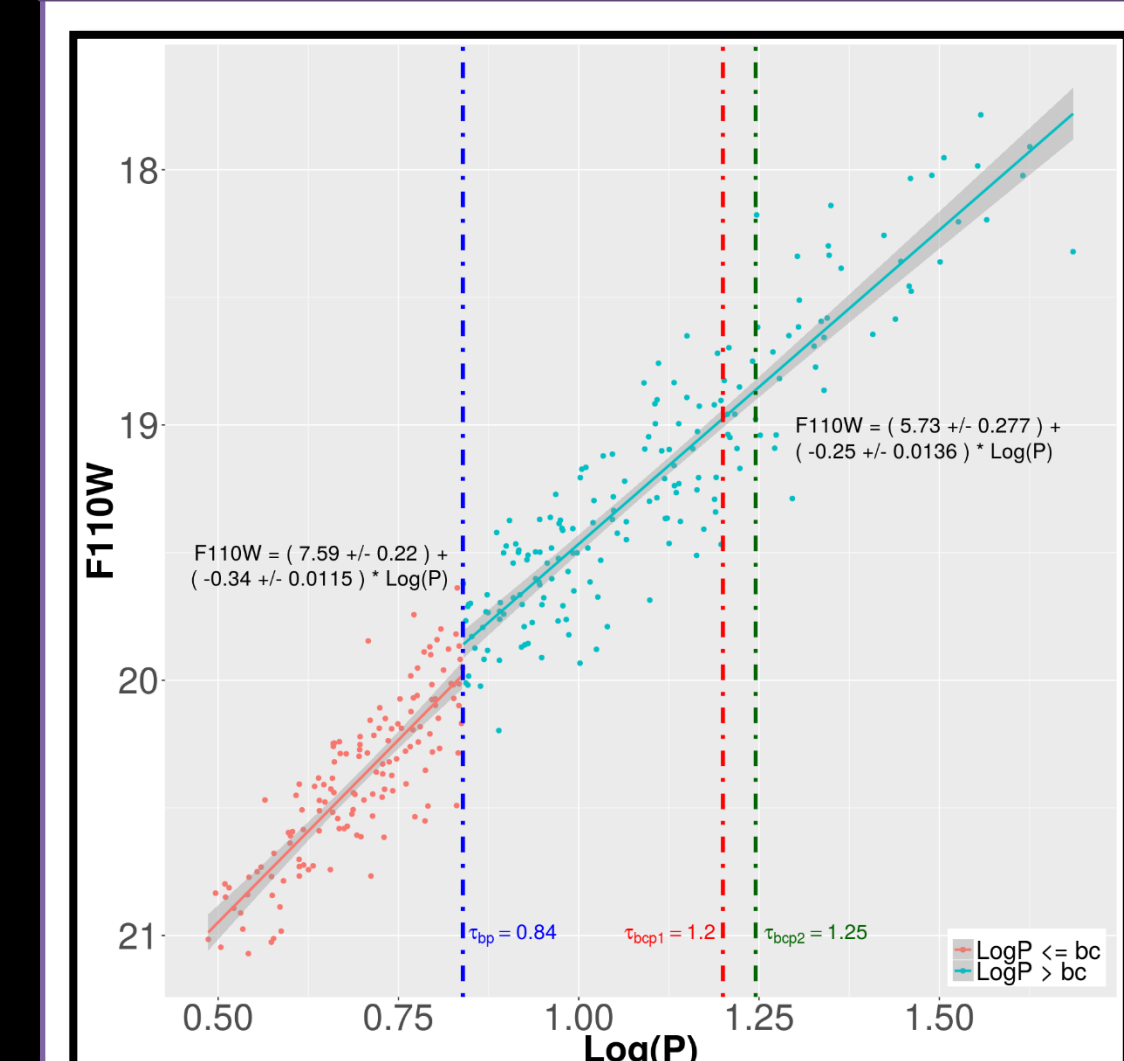


Figure 6 – Breaking points found for Fundamental Mode Cepheids in M31 (Kodric et al. , 2015). It is important to note that while the mean value of breaking point found by bcp is close to 1.25, bcp finds also significant posterior probabilities for a breaking point nearing 0.85, hence we decide to use the value found by BP to build our fitting functions.

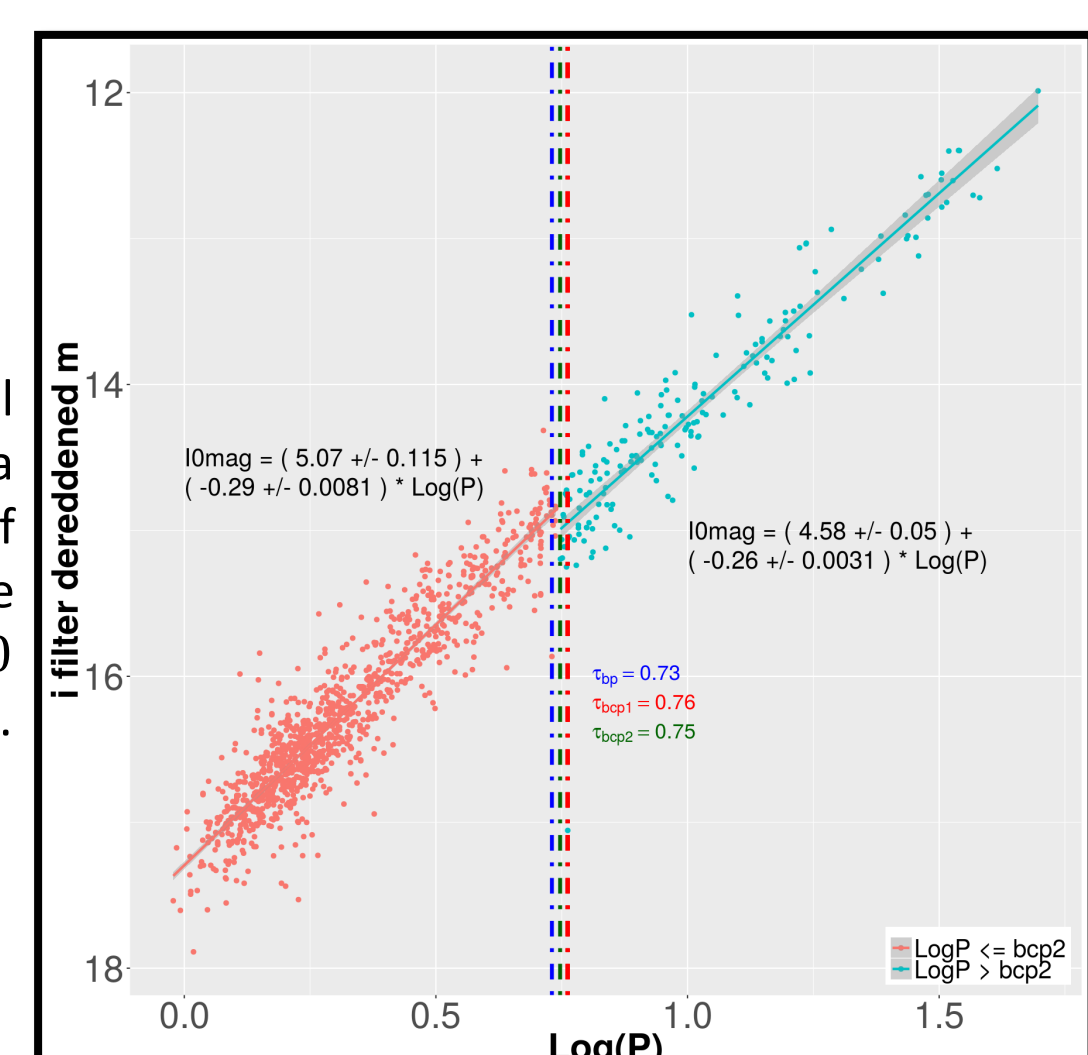


Figure 7 – Breaking points found for Fundamental Mode Cepheids in the SMC, from OGLE data (Udalski et al. , 1999). The large distribution of magnitudes, the presence of outliers and the small number of stars with $P > 10 \text{ d}$ (only ~ 100 in a sample of 1319) can explain the values found.

Figure 8 – Breaking points found for Fundamental Mode Cepheids, in the LMC, from MACHO project (2001). The bp method failed to identify a breaking point while bcp1 and bcp2 found one each but with low confidence. In this sample also, the strong dispersion of data and the lack of long period Cepheids are probable explanations.

- Applications of the BP and bcp methods to real samples give mixed results.
- With Kodric et al. (2015), the BP method finds a breaking point at $P \approx 6.9 \text{ d}$ and the bcp methods at $P \approx 17 \text{ d}$ (figure 6).
- With Udalski et al. (1999), a breaking point is found by all methods at $P \approx 5.6 \text{ d}$ (figure 7).
- Using data from the MACHO project (2001), the method bcp1 find a breaking point at $P \approx 4.5 \text{ d}$ and bcp2 at $P \approx 5.6 \text{ d}$ (figure 8).
- All samples show a large distribution of values of magnitudes and an unbalanced number of stars on each side of the $P = 10 \text{ d}$ expected breaking point. Fitting functions on each side of the breaking points found fail to offer a better description of the function than the regular linear function.

6. Conclusions and further investigations

- Both BP and bcp methods have shown efficiency in the simulated data up to $\sigma = 0.4$.
- Both BP and bcp methods behaved as expected on the chosen samples of observational data. There is a strong need for caution, since the breaking points found may have different origins than the non-linearity of the LL in these specific cases.
- These statistical methods require further investigation as the accuracy of photometric measurements and calculation of Cepheids periods are constantly improving.
- Future work will include:
 - i. A more refined selecting protocol for samples of stars.
 - ii. Investigation of more breaking point algorithms.
 - iii. Experimenting on the most recent data from the POMME survey which contains a larger sample of stars with high photometric accuracy.

7. References

Bai & Perron 2003, JAE, 18, 1 — Barry & Hartigan 1993, JASA, 88, 309 — Caputo et al. 2000, A&A, 359, 1059C — Erdman & Emerson 2007, JSS, 23, 03 — Kodric et al. 2015, AJ, 799, 144K — MACHO Project — Marconi et al. 2005, AJ, 632, 590M — Ngeow & Kanbur 2009, ASPC, 404, 262N — Ngeow et al. 2005, MNRAS, 363, 881N — Ngeow et al. 2008, A&A, 477, 621N — Riess et al. 2012, AJ, 745, 156R — Tammann et al. 2002, ASPC, 283, 258T — Udalski et al. 1999, AcA, 49, 437

Acknowledgements: we would like to thank Anne-Laure Melchior and Gerard Gregoire.